

NISTIR 7592

Study of Acid Generation from Copolymer Fibers based on 5-amino-2-(*p*-aminophenyl)- benzimidazole

Amanda L. Forster, Guillaume H. R. Messin, Kirk D. Rice,
Michael A. Riley, and Stephanie S. Watson



NISTIR 7592

Study of Acid Generation from
Copolymer Fibers based on
5-amino-2-(*p*-aminophenyl)-
benzimidazole

Amanda L. Forster, Guillaume H. R. Messin,
Kirk D. Rice, Michael A. Riley
Office of Law Enforcement Standards
Electronics and Electrical Engineering Laboratory

Stephanie S. Watson
Materials and Construction Research Division
Building and Fire Research Laboratory

September 1, 2009



U.S. Department of Commerce
Gary Locke, Secretary

National Institute of Standards and Technology
Patrick D. Gallagher, Deputy Director

Abstract

In a communication to the ballistic vest community released in January 2006, there was an allegation by a competing fiber manufacturer that copolymer fibers based on 5-amino-2-(*p*-aminophenyl)-benzimidazole can release hydrochloric acid, which could potentially be detrimental to other fibers that might come in contact with these materials. Despite the fact that these allegations came from a competing manufacturer, this issue was investigated to determine if it was an officer safety issue. This study investigates the evolution of acid in aqueous environments from these fibers, reviews the available literature on the fibers, and provides an analysis of the chemical structure of these fibers to serve as the basis for future studies. It was determined that there is some evidence to support the allegations; two of the fiber samples studied released a sufficient amount of acid to drop the pH of an aqueous solution from approximately pH 6.0 to approximately pH 3.0 in less than ten days. Further ion-selective electrode (ISE) studies of chloride ion released from these fibers indicated that hydrochloric acid may not be the species responsible for this pH reduction. Future studies are planned to better elucidate the species responsible for this pH reduction and examine the effect of moisture on the pH reduction of the fibers, as well as the effect of water vapor on the chemical and physical properties of these fibers.

This page intentionally left blank.

Acknowledgments

Financial support for this research effort was provided by the National Institute of Justice under Interagency Agreement Number 2003-IJ-R-029. Their support is gratefully acknowledged.

This page intentionally left blank.

Disclaimer

Certain commercial equipment, instruments, or materials are identified in this paper in order to specify the experimental procedure adequately. Such identification is not intended to imply recommendation or endorsement by the National Institute of Standards and Technology, nor is it intended to imply that the materials or equipment identified are necessarily the best available for this purpose.

This page intentionally left blank.

Contents

1	Introduction	1
2	Background	5
2.1	Fiber Manufacture	5
2.2	Structure and Physical Properties	5
2.3	Moisture Sorption and Other Properties	7
2.4	Suitability for Ballistic Applications	8
2.5	Acid Generation	8
3	Experimental	11
3.1	Fiber Exposure to Aqueous Environments	11
3.2	Infrared Spectroscopy Measurements	11
4	Results and Discussion	13
4.1	Chloride Ion Concentration and pH Measurements	13
4.2	Analysis of Chemical Structure	17
5	Conclusions and Future Work	19
6	References	29

This page intentionally left blank.

List of Tables

5.1 Infrared peak assignments for all fibers studied. 22

This page intentionally left blank.

List of Figures

1.1	Basic chemical structure of the copolymer fibers (Armos, Rusar, and Artec).	3
1.2	Basic chemical structure of PPTA fibers.	3
1.3	Basic chemical structure of SVM fibers.	3
2.1	Schematic of spinning process for the copolymer fibers.	6
2.2	Characteristic moisture sorption isotherms for PPTA and the copolymer fibers	7
4.1	Change in pH following immersion in deionized water.	14
4.2	Chloride ion generation following immersion in deionized (DI) water for all fibers.	15
4.3	Chloride ion generation following immersion in deionized (DI) water for all fibers except SVM.	16
5.1	ATR FT-IR spectrum of virgin Armos fiber.	23
5.2	ATR FT-IR spectrum of virgin Artec fiber.	24
5.3	ATR FT-IR spectrum of virgin Rusar fiber.	25
5.4	ATR FT-IR spectrum of virgin SVM fiber.	26
5.5	ATR FT-IR spectrum of virgin PPTA fiber.	27

This page intentionally left blank.

1. Introduction

Modern body armor utilizes a wide range of polymers to provide the level of performance required for these applications. The materials most commonly utilized in body armor are poly(*p*-phenylene terephthalamide) (PPTA) and the ultra-high molecular weight polyethylenes (UHMWPE); however, in an effort to provide additional consumer choices, several additional fibers have been recently introduced into the United States body armor marketplace. These fibers were developed in the former USSR in the late 1970s, and are based on several starting monomers [1]. Several of these fibers were investigated in this study, including Artec, Rusar, SVM, and Armos. PPTA fiber was used as a comparison fiber. Artec, Rusar, and Armos all have the same basic chemical composition, as depicted in Figure 1.1, and are formed by polycondensation reaction of two diamines, *p*-phenylene diamine and 5-amino-2-(*p*-aminophenyl)-benzimidazole with terephthalic acid (or anhydrides or acid chloride derivatives of these monomers). PPTA fibers, sold under trade names Kevlar and Twaron, are manufactured by polycondensation of *p*-phenylenediamine with terephthalic acid. The structure of PPTA fibers is shown in Figure 1.2. For the purposes of this work, linkages between terephthalic acid and 5-amino-2-(*p*-aminophenyl)-benzimidazole will be referred to as *benzimidazole linkages* and linkages between *p*-phenylene diamine and terephthalic acid will be referred to as *PPTA linkages*.

The main difference between these fibers is the ratio of benzimidazole linkages to PPTA linkages [2]. While specific information on these ratios is difficult to obtain, one weaver of these fibers supplied information indicating that in the case of Artec, the ratio of PPTA to benzimidazole linkages was 2:1, and in the case of Rusar, the ratio of diamine to benzimidazole linkages was 1:1. Additionally, Rusar is made with raw materials sourced from Eastern Europe, and Artec is made with raw materials sourced from the United States [3]. Another fiber that was investigated in this study is sold under the trade name SVM. This homopolymer fiber is manufactured by direct polycondensation of 5-amino-2-(*p*-aminophenyl)-benzimidazole with terephthalic acid [4]. The structure of SVM fiber is shown in Figure 1.3.

In a communication to the body armor community released in January 2006, there was an allegation by a competing fiber manufacturer that copolymer fibers based on 5-amino-2-(*p*-aminophenyl)-benzimidazole can release

hydrochloric acid, which could potentially be detrimental to other fibers that might come in contact with these materials [5]. Despite the fact that these allegations came from a competing manufacturer, due to recent issues with degradation of another fiber in field use, it was determined that this allegation should be investigated to determine if it was an officer safety issue.

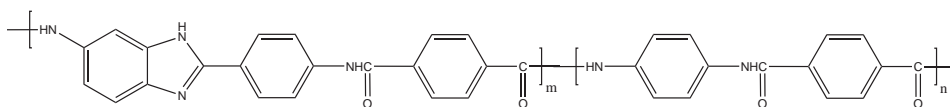


Figure 1.1: Basic chemical structure of the copolymer fibers (Armos, Rusar, and Artec).

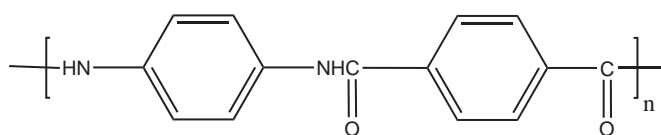


Figure 1.2: Basic chemical structure of PPTA fibers.

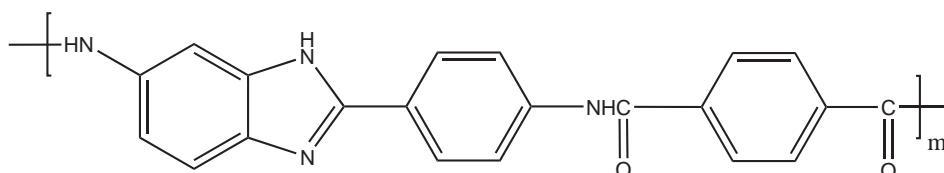


Figure 1.3: Basic chemical structure of SVM fibers.

This page intentionally left blank.

2. Background

2.1 Fiber Manufacture

While details of the specific processes by which these fibers are made is difficult to find in the literature, a general idea of the fabrication of Armos fiber can be determined from a paper published by Machalaba et al., in 2000. One can readily assume that the general processing steps would apply to the other fibers as well. The homopolymer (SVM) or copolymer (Armos, Rusar, Artec) is manufactured by polycondensation of terephthalic acid chloride and some combination of para-aromatic diamines (*p*-phenylene diamine or 5-amino-2-(*p*-aminophenyl)-benzimidazole) in an amide-salt solvent system (specified as dimethylacetamide and lithium chloride in the Machalaba paper). The polymer formed from this reaction is then filtered and degassed prior to being spun into a filament yarn. This yarn is then drawn and heat treated to form the final finished product. Dyeing and twisting can also be performed, if necessary, after the spinning step. A schematic of this process is shown in Figure 2.1 [6].

2.2 Structure and Physical Properties

Slugin et al., published two papers in 2006 related to the use of Rusar fibers for composites and ballistic protection applications. In one of these papers, they disclose the information discussed in Section 1 regarding the structure and monomers of this fiber [4, 7]. Additional information is given regarding the rationale for use of the co-monomer 5-amino-2-(*p*-aminophenyl)-benzimidazole. The authors state that the incorporation of this second diamine in the Rusar fibers significantly alters the rigidity of the polymer chain (as is evident from an analysis of the slight nonlinearity in the polymer backbone), as compared to PPTA fibers. This decreases the ability of the polymer to form a lyotropic liquid crystalline spinning solution because the molecule is not capable of forming a highly organized structure, leading to a reduced overall crystallinity. However, this reduced crystallinity allows for additional organization of the amorphous portions of the Rusar fiber during post-spinning drawing and heat treatment [4]. This work is supported by a paper from Zavadskii et al., in which the structure of Armos and SVM were investigated using X-ray diffraction, and evidence was found to indi-

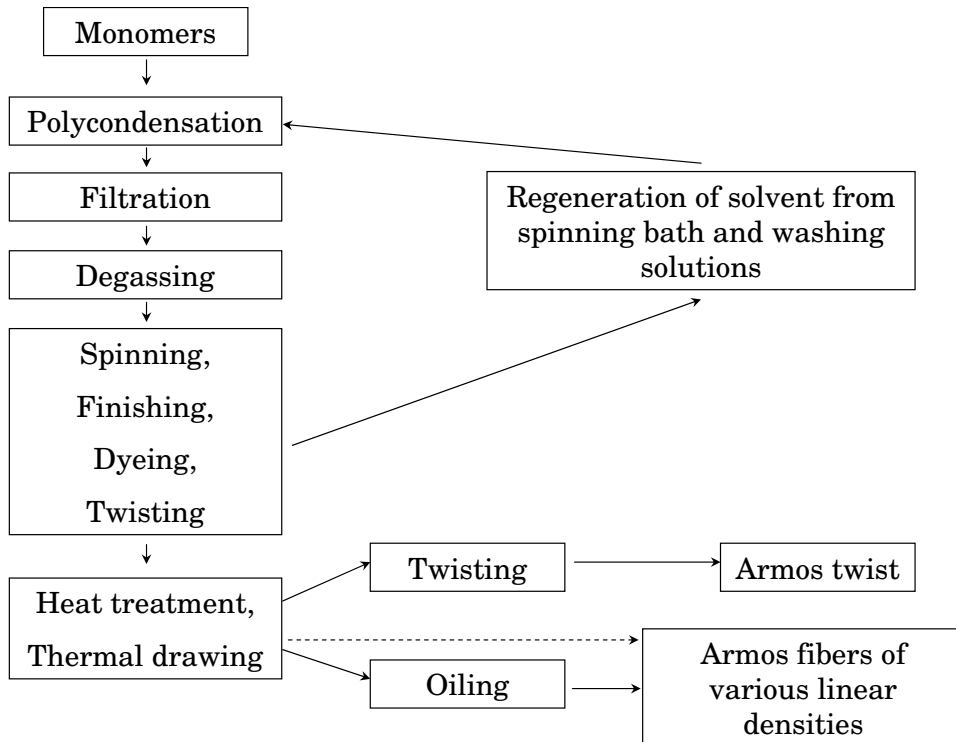


Figure 2.1: Schematic of spinning process for the copolymer fibers.

cate the absence of rigorous order in the position of the molecular chains in the direction perpendicular to the axis of the fiber [8]. A paper published by Perepelkin in 2001 compares the properties of Armos and SVM with commercial polyamide yarns. The primary difference between these fibers is in their structural properties. Polyamide fibers have a fibrillar structure with stretched chains and three-dimensional order. SVM fibers also have a fibrillar structure with stretched chains, but only one-dimensional crystalline order. The Armos fiber, one of the copolymer fibers, has a fibrillar structure with stretched chains, but no crystalline order. The strength at break of the Armos fiber is reported at 4.5 GPa to 5.5 GPa as compared to 2.7 GPa to 3.5 GPa for the polyamide fibers, leading the authors to conclude that crystallinity is not a prerequisite for preparing fibers with good mechanical properties [9]. It appears that the Armos fiber has been investigated for use in composite applications due to its unique transverse mechanical properties. A paper by Leal et al., from 2007 attributes the lack of three-dimensional organization in Armos fiber to the ability to achieve greater draw ratios, better molecular orientation, and improved mechanical properties. Additionally, Armos develops intermolecular hydrogen bonds that allow for stress transfer between adjacent chains. This improves the compressive properties of the fiber and makes it attractive for use in composite applications [2, 10].

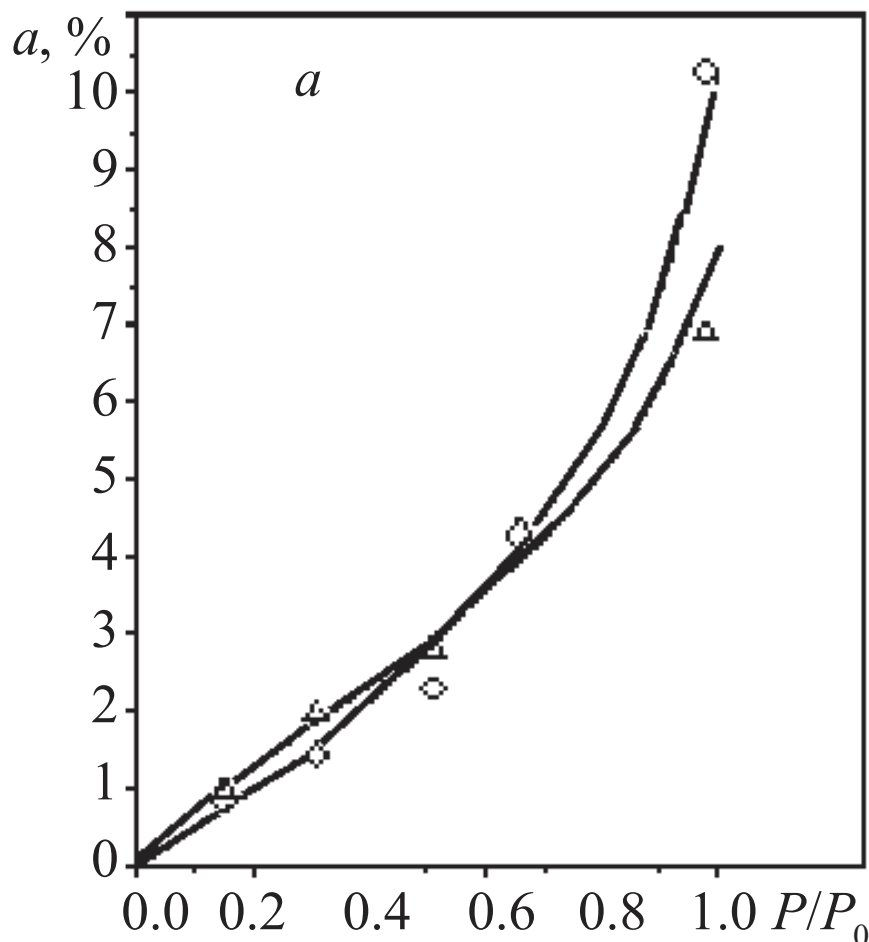


Figure 2.2: Characteristic moisture sorption isotherms for PPTA (triangles) and the copolymer (diamonds) fibers [12].

2.3 Moisture Sorption and Other Properties

Studies on the moisture sorption properties of several fibers as compared to PPTA have shown that Rusar has very similar sorption isotherms to PPTA, as shown in Figure 2.2. Differences in the sorption properties of these materials are attributed to the lower crystallinity of SVM and Rusar as compared with PPTA. As previously discussed, the benzimidazole linkages in these polymers do not crystallize as readily as do the more linear polyamide linkages [11, 12].

Much work [13, 14, 15, 16] has been performed to investigate the thermal stability of these fibers for use in high-temperature environments and fire applications. These materials are chemically similar to other fibers used in fire-resistant applications, such as *para* and *meta*-aramid fibers, so interest in their thermal properties is not surprising. The decomposition tempera-

tures in air for Armos showed that it was stable to oxidation and onset of degradation to approximately 400 °C [15]. A separate study on the thermal stability of PPTA, SVM, Rusal, and Armos fibers in which the fibers were exposed to 250 °C for periods of time between 0 h and 100 h showed that the mechanical properties of the SVM fibers decreased the most rapidly, and that there was little difference in the thermal stability of the other fibers examined [13].

2.4 Suitability for Ballistic Applications

The authors present V_{50} data on ballistic packages manufactured from two different linear densities of Rusal yarn to demonstrate the appropriateness of this material for ballistic applications. The authors report a V_{50} of 640 m/s and 550 m/s for packages made from microfilament yarn fibers with linear densities of 29.4 tex (264.6 denier) and 58.8 tex (529.2 denier), respectively [7]. It is important to note several omissions in the presentation of this data. No details were provided as to the areal density of the ballistic packages created, no details were provided as to the characteristics of the ballistic fabrics used, and no mention was made of the number of layers of fabric used to make the ballistic packages, making it difficult to draw meaningful conclusions from these results.

2.5 Acid Generation

A paper published by Shchetinin et al., in 2006 attempted to address the allegations raised by the competitive fiber manufacturer about the evolution of acid from these fibers. In this paper, it is revealed that hydrochloric acid is a by-product in the synthesis of the polymer, but most of the acid is removed when the fiber is washed after spinning and heat treatment [17]. The acidity of the finished fiber is also discussed in a paper from 1995 by Kotomin et al., which indicated that the pH of the fiber varied with heat treatment conditions to between 3.5 and 6.5, as determined by titration of an aqueous extract of the fiber [10]. There is a residual amount of acid (0.1 % to 2.5 % of the fiber's mass) chemically bound to the amide and imidazole groups in the fibers. This amount of bound acid is greatest for the SVM fibers, indicating that it is a by-product of synthesis with the 5-amino-2-(*p*-aminophenyl)-benzimidazole and the terphthalic acid or anhydrate. The authors used SVM yarns for their study, and in the paper indicate that the amount of bound HCl in the Armos and Rusal copolymer fibers is less than 0.2 %. SVM fiber samples with an initial hydrochloric acid content of 1.5 % were stored in sealed flasks with deionized water at a ratio of 1 part fiber to 10 parts water, and the pH of the water in solution was periodically evaluated after storage at 15 °C to 25 °C. The pH of the extract decreased from 6.4 initially to 4.8 after 360 d of storage under these conditions. The authors conclude that this is an insignificant change in the pH of the water over this period of time. They also indicate that since the acid content of the Rusal/Artek (in this paper they use Rusal and Artek/Artek interchangeably,

leading to the conclusion that these fibers are chemically very similar) and Armos is so low, that this is not an issue for these fibers; however no data is offered to support this conclusion [17].

This page intentionally left blank.

3. Experimental

The principal objective of this study is to evaluate the amount of chloride released from Rusal, Armos, Artec, SVM, and PPTA fibers while exposed to water in a liquid or gas state. Fibers were immersed in deionized water for a specified period of time, and the pH and chloride ion content of the water were measured over time using ion-selective electrodes. Infrared analysis was performed on the unexposed fibers to assist in verification of their structure and will form a basis for future studies of the effect of exposure to water on their chemical structure.

3.1 Fiber Exposure to Aqueous Environments

As mentioned previously, during the first part of this study, chlorine emission and pH were monitored by ion-selective electrodes as a function of time under controlled conditions on fibers submerged in deionized water. Fiber samples of the Armos, Artec (removed from a fabric sample), Rusal, SVM, and PPTA (removed from a fabric sample) weighing 5 g, were immersed in 500 mL of deionized water for 10 d and measured at specified intervals. Previous studies in our laboratory had shown that, after 10 d, no further changes in pH or chlorine emission were observed. The beakers were kept tightly sealed with paraffin wax film except when measurements were being made. The total volume of water was kept constant in the beakers by addition of deionized water, if necessary, over the course of the experiment. The generation of chloride ions into solution and solution pH were monitored using a Fisher Scientific Accumet Excel XL50 multichannel meter with a chloride combination ion-selective electrode (ISE) and a pH electrode. The standard uncertainty for the pH electrode is ± 0.1 pH units, and the standard uncertainty is ± 0.2 % for the ion-selective electrode [18].

3.2 Infrared Spectroscopy Measurements

Infrared analysis was carried out using a Bruker Vertex 80 Fourier Transform Infrared Spectroscopy (FTIR), equipped with a Smiths Detection Durascope Attenuated Total Reflectance (ATR) accessory. Dry air was used as the purge gas. Constant pressure on the yarns was applied using the force monitor on the Durascope. FTIR spectra were recorded at a resolution of 4

cm^{-1} between 4000 cm^{-1} and 600 cm^{-1} and averaged over 128 scans. Three different locations on each yarn were analyzed. Standard uncertainties associated with this measurement are typically $\pm 4 \text{ cm}^{-1}$ in wavenumber and 1 % in peak intensity [19].

4. Results and Discussion

4.1 Chloride Ion Concentration and pH Measurements

Representative pH and chloride ion concentration measurements as a function of time are shown in Figure 4.1 through Figure 4.3. The most rapid changes in both pH and chloride ion concentration occur in the first five days of liquid water exposure. The change was greatest for the SVM yarn, which is expected due to the high chlorine content of this yarn [17]. The change in pH as a function of immersion time is shown in Figure 4.1. The SVM and Rusar fibers showed a pH decrease from approximately pH 6.0 to approximately pH 3.0. Artec showed the smallest change in pH as a function of time, with a reduction to approximately pH 5.5 in 10 d. Armos and PPTA showed a decrease in pH from approximately pH 6.0 to pH 4.5.

As would be expected from the pH results, SVM showed the greatest increase in overall chloride ion concentration, as shown in Figure 4.2. The overall increase was from almost zero mg/L chlorine in solution up to 158 mg/L chlorine in solution for the SVM yarn. Interestingly, this trend is not mimicked by the Rusar fiber, indicating that another species may be responsible for its drop in pH. In an effort to better separate the scale, the chloride ion results obtained for the Artec, PPTA, Armos, and Rusar fibers are replotted in a separate graph, Figure 4.3. None of the other fibers investigated exhibited a significant change in the chloride ion concentration. One may note that the pH of the deionized water control is approximately 6.0. We attribute this lower-than-expected pH to the well-known formation of weak carbonic acid in deionized water after exposure to carbon dioxide in the air [20]. The water deionizer source used for these experiments stores the deionized water in a large reservoir as it is made, so the water is exposed to air, and carbon dioxide, for a long time before use, allowing for ample formation of carbonic acid. We believe that the presence of the carbonic acid in solution may contribute to the removal of chloride ions from some of the fibers in solution. Though further chemical analysis will be necessary to confirm this hypothesis, one can surmise that the source of the chloride ion is residual ammonium chloride formed from the reaction of terephthalic acid chloride and the primary or secondary amines to form the polymers studied herein. The polycondensation reaction of the amine and the acid

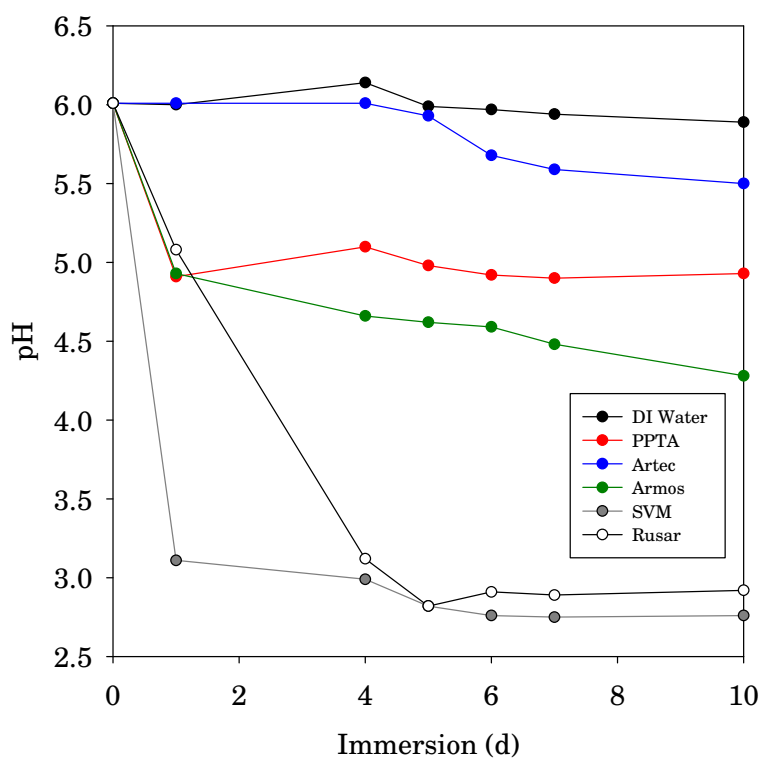


Figure 4.1: Change in pH following immersion in deionized (DI) water. The low pH value observed for deionized water is probably due to the formation of carbonic acid in deionized water after exposure to carbon dioxide in the air.

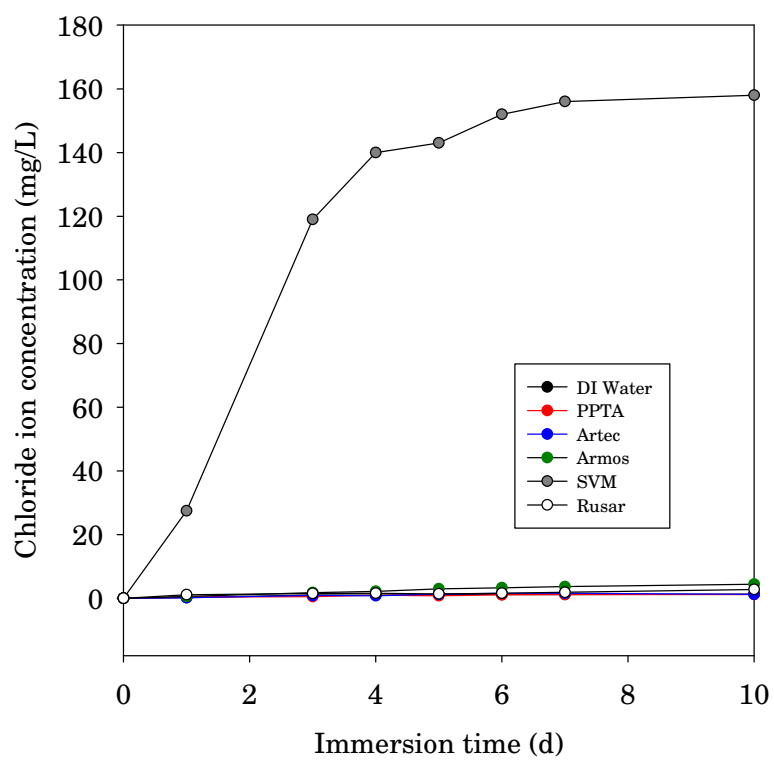


Figure 4.2: Chloride ion generation following immersion in deionized (DI) water for all fibers.

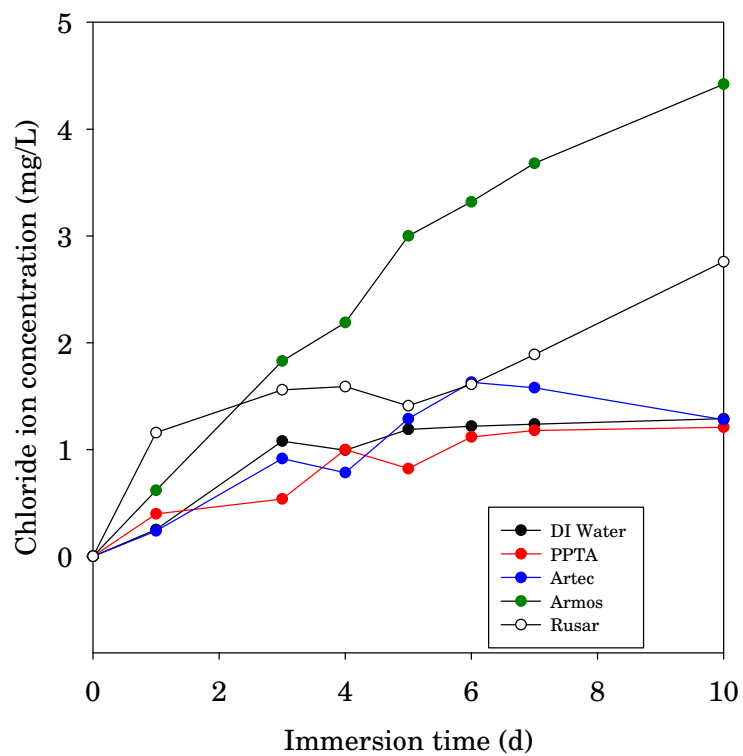


Figure 4.3: Chloride ion generation following immersion in deionized (DI) water for all fibers except SVM.

chloride to form the amide bond will result in the small molecule byproduct HCl. The nitrogen in the amide bond has a lone pair of electrons that can react with the HCl to form the ammonium chloride ion pair. Traces of this salt may remain after thorough washing of the fibers, and when the polymer is immersed in water for these studies, small amounts of chloride ion may be gradually released from the polymer. The carbonate ion could displace some of the chloride ion associated with the ammonium salt, thereby increasing the chloride ion concentration in the solution and contributing to the increasing levels of chloride ion detected in this study, and also potentially forming HCl in solution. Future studies are planned to examine this phenomenon.

4.2 Analysis of Chemical Structure

Due to the apparent lack of available literature regarding the infrared analysis of the chemical structure of the copolymer fibers utilized in this study, a separate effort was undertaken to investigate their spectra. This will form the basis of work to examine the effect of moisture exposure on the chemical structure of these fibers, which will be the subject of a forthcoming report. Peak assignments were generated through the review of several references on PPTA fibers [21, 22], general infrared spectroscopy [23, 24, 25], and benzimidazole spectroscopy [26, 27]. The results of this analysis are presented in Table 1. Representative ATR FT-IR spectra for all fibers studied are presented in the Appendix. As expected, the spectra of the copolymer fibers show characteristics found in the spectra of the two homopolymers. No information related to relative copolymer ratios for the different fibers could be determined from this analysis, but this may be a subject of future work.

This page intentionally left blank.

5. Conclusions and Future Work

All fibers studied herein, even PPTA, emit some quantity of acid when immersed in liquid water. However, the pH drop for the fibers SVM and Rusar was greater than that observed for the other fibers. The theory that hydrochloric acid is responsible for this reduction in pH may only be true for the SVM fibers, as these fibers were the only ones that exhibited an increase in chloride ion concentration to correspond to the reduction in pH. This leads us to the conclusion that another type of acid must be responsible for the pH reduction in the Rusar sample. Elemental analysis via X-ray fluorescence (XRF) of all the fibers in this study will be performed in a future study to estimate the concentration of chlorine in the samples, and possibly further elucidate the species responsible for the pH reduction, especially in the Rusar sample. Additionally, studies to examine whether exposure to water vapor has the same effect on pH as liquid water are currently underway, as these studies better represent the use environment for body armor. These results will be the subject of a future publication. Finally, a study to examine the effect of exposure to water in both its liquid and vapor form on the chemical and physical properties of these fibers will be performed to determine if these fibers have any of the vulnerabilities to hydrolysis that have become apparent in other commercial fibers used in body armor.

This page intentionally left blank.

Appendix

STUDY OF ACID GENERATION FROM COPOLYMER FIBERS BASED ON
5-AMINO-2-(*p*-AMINOPHENYL)-BENZIMIDAZOLE

Artec	Wavenumber (cm ⁻¹)				Note	General Assignment
	Armos	Rusar	SVM	PPTA		
				3309	Broad	NH Stretch [22]
3271	3271	3271			Broad	Imidazole NH proton hydrogen bonding to water molecules or nearby imine [26]
2917	2917	2916	2925	2916	Weak	Aromatic CH stretch [24]
2849	2849	2855	2848	2848	Weak	Aromatic CH stretch [24]
1638	1639	1638	1632	1638	Strong	Amide I band carbonyl [21]
1596	1596	1596	1593		Shoulder	Benzimidazole NH in plane bend [27]
				1537	Sharp Shoulder	Amide II band carbonyl [21]
			1525		Sharp Shoulder	Aromatic CH stretch [24]
1513	1512	1513		1510	Sharp Shoulder	Amide II band carbonyl [21]
1487	1486	1488	1488		Shoulder	Benzimidazole ring stretch [27]
	1467		1464		Shoulder	Benzimidazole ring stretch [27]
1443	1443	1443	1443		Shoulder	Benzimidazole [27]
			1417		Shoulder	Benzimidazole ring stretch [27]
1406	1406	1406		1394	Shoulder	Primary amine salts [24]
1305	1304	1304	1300	1303	Shoulder	CN stretch; Amide III group motion [22]
1244	1245	1247	1244		Shoulder	Benzimidazole ring stretch [27]
1187	1186	1186	1186		Medium	Benzimidazole in-plane CH bend [27]
1108	1107	1108	1106	1107	Medium	Benzimidazole in-plane CH bend [26]
1016	1016	1016	1015	1017	Medium	CH out of plane bend [22]
957	957	955	957		Weak	Imidazole in plane bend [27]
890	889	890	889	893	Weak	CH out of plane [21]
862	862	862	861	862	Shoulder	Unassigned
				820	Strong	CH out of plane [22]
808	808	808	806		Broad, Medium	Unassigned
				820	Strong	CH out of plane [22]
712	712	712	712		Broad, Shoulder	Unassigned
689	689	689	689		Shoulder	Unassigned
608	609	608	609		Shoulder	Unassigned

Table 5.1: Infrared peak assignments for all fibers studied.

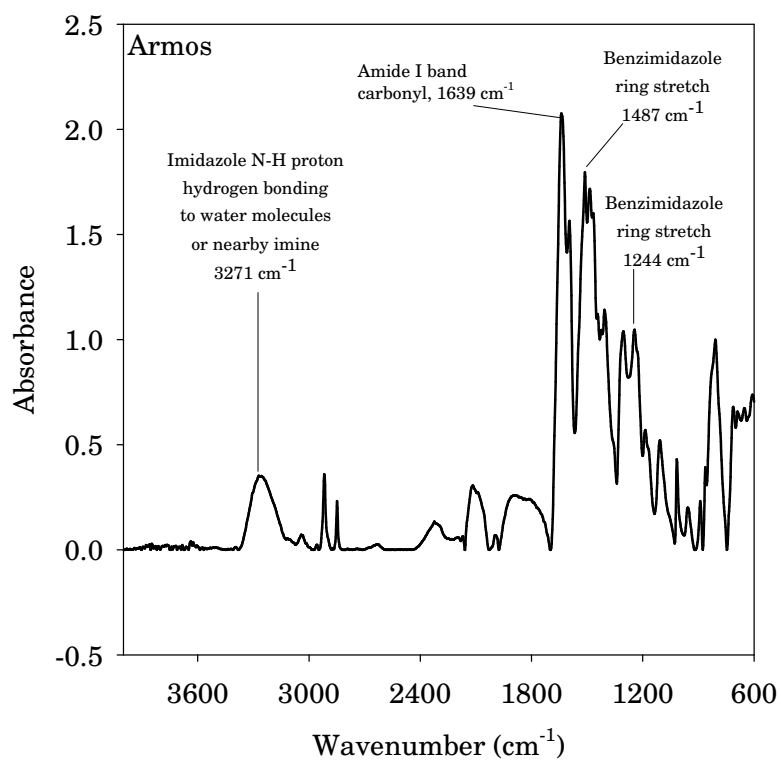


Figure 5.1: ATR FT-IR spectrum of virgin Armos fiber.

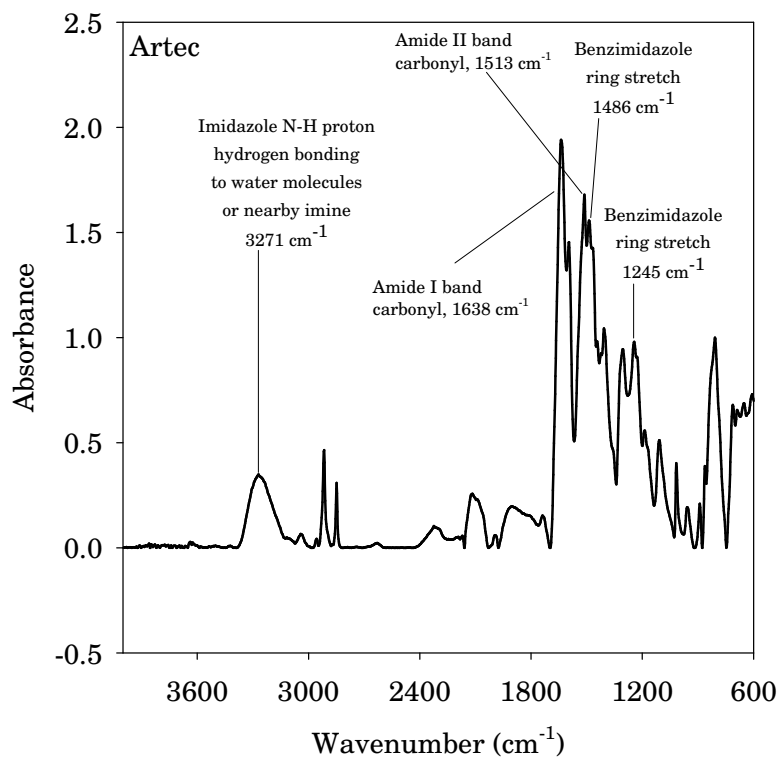


Figure 5.2: ATR FT-IR spectrum of virgin Artec fiber.

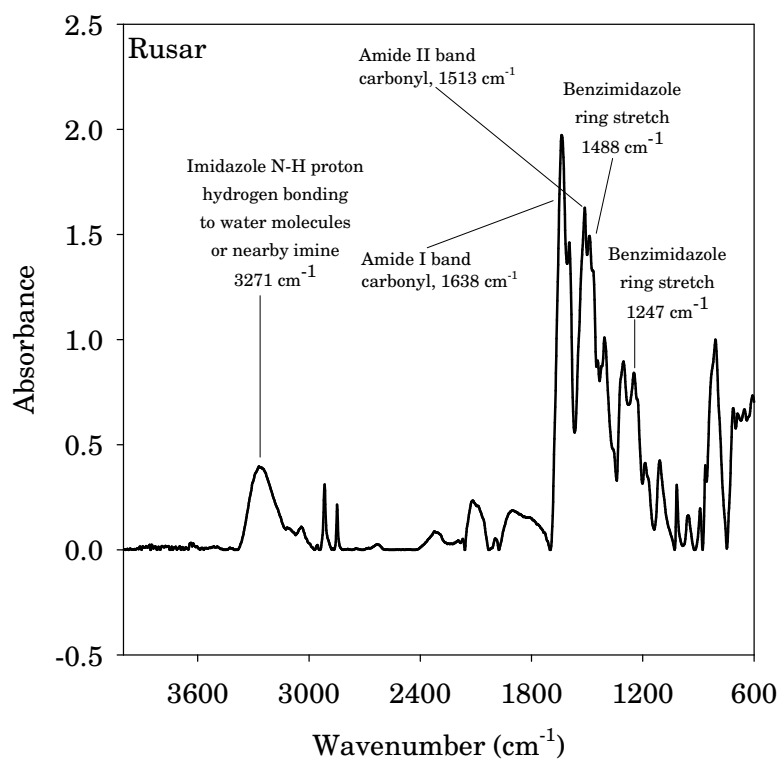


Figure 5.3: ATR FT-IR spectrum of virgin Rusar fiber.

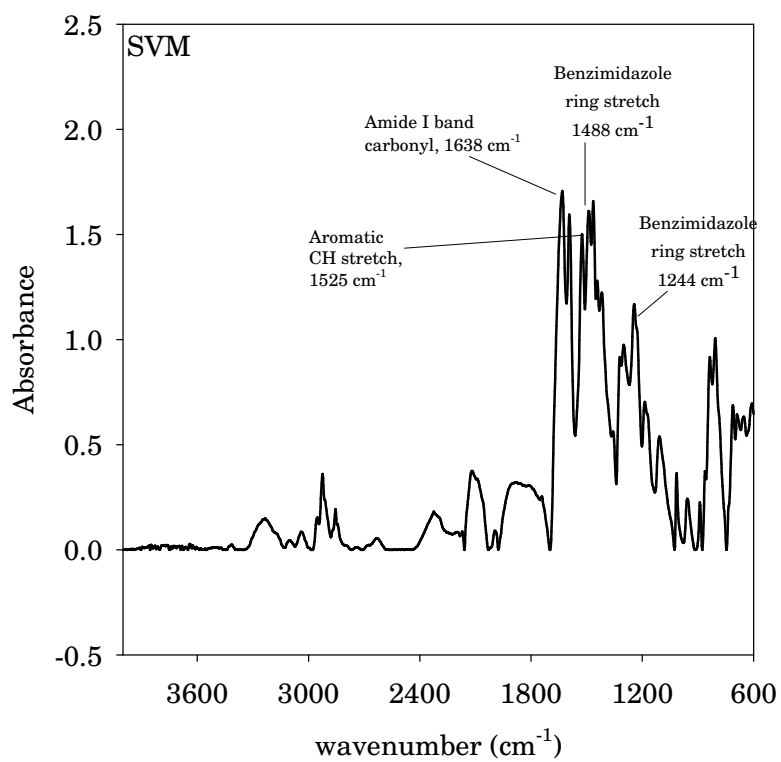


Figure 5.4: ATR FT-IR spectrum of virgin SVM fiber.

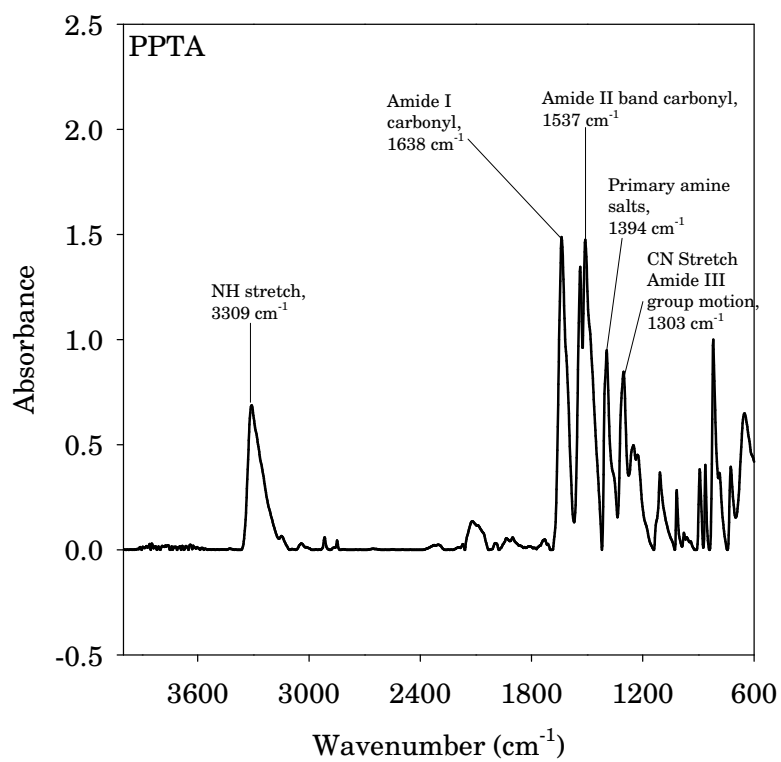


Figure 5.5: ATR FT-IR spectrum of virgin PPTA fiber.

This page intentionally left blank.

6. References

- [1] J. W. S. Hearle. *High Performance Fibers*. Woodhead Publishing, Cambridge, 2001.
- [2] A. A. Leal, J. M. Deitzel, and J. W. Gillespie. Assessment of compressive properties of high performance organic fibers. *Composites Science and Technology*, 67(13):2786–2794, 2007.
- [3] Artec fiber vs rusar fiber technical differences (as per yarn manufacturer communication), 2006.
- [4] I. V. Slugin, G. B. Sklyarova, A. I. Kashirin, and L. V. Tkacheva. Rusar para-aramid fibres for composite materials for construction applications. *Fibre Chemistry*, 38(1):25–26, 2006.
- [5] David Hand. Hybrid vests made from twaron fibers and co-polymer aramid yarns containing 5-amino-2-(p-aminophenyl)-benzimidazole or related monomers, January 2006.
- [6] N. N. Machalaba, N. N. Kuryleva, L. V. Okhlobystina, P. A. Matytsyn, and I. A. Andriyuk. Tver’ fibres of the armos type: Manufacture and properties. *Fibre Chemistry*, 32(5):319–324, 2000.
- [7] I. V. Slugin, G. B. Sklyarova, A. I. Kashirin, L. V. Tkacheva, and S. V. Komissarov. Rusar microfilament yarn for ballistic protection. *Fibre Chemistry*, 38(1):22–24, 2006.
- [8] A. E. Zavadskii, I. M. Zakharova, and Z. N. Zhukova. Features of the fine structure of aramid fibres. *Fibre Chemistry*, 30(1):6–10, 1998.
- [9] K. E. Perepelkin, N. N. Machalaba, and V. A. Kvaratskheliya. Properties of armos para-aramid fibres in conditions of use. comparison with other para-aramids. *Fibre Chemistry*, 33(2):105–114, 2001.
- [10] S. V. Kotomin, A. A. Basharov, V. G. Bova, and E. M. Sapozhnikov. Realization of the strength of armos fibres with different acidity in epoxy plastics. *Fibre Chemistry*, 28(1):48–49, 1996.
- [11] S. F. Grebennikov, T. V. Smotrina, N. P. Lebedeva, and K. E. Perepelkin. Molecular mobility in the superstrong para-aramid fibre-water system. *Fibre Chemistry*, 40(3):206–207, 2008.

- [12] K. E. Perepelkin, S. F. Grebennikov, and N. P. Lebedeva. Sorption of water vapors by high-strength para-aramid fibres. *Fibre Chemistry*, 39(5):420–423, 2007.
- [13] K. E. Perepelkin, I. V. Andreeva, G. P. Meshchervakova, and I. Y. Morgoeva. Change in the mechanical properties of para-aramid fibres in thermal aging. *Fibre Chemistry*, 38(5):400–405, 2006.
- [14] K. E. Perepelkin, I. V. Andreeva, E. A. Pakshver, and I. Y. Morgoeva. Thermal characteristics of para-aramid fibres. *Fibre Chemistry*, 35(4):265–269, 2003.
- [15] K. E. Perepelkin, O. B. Malan'ina, E. A. Pakshver, and R. A. Makarova. Comparative evaluation of the thermal properties of aromatic fibres (polyoxazole, polyimide, and polyaramid). *Fibre Chemistry*, 36(5):365–369, 2004.
- [16] V. A. Platonov, G. G. Frenkel, and A. M. Shchetinin. X-ray study of the effect of heat on the structural parameters of armos fibres. *Fibre Chemistry*, 35(4):283–286, 2003.
- [17] V. M. Shchetinin, I. V. Tikhonov, and A. V. Tokarev. The pseudoeffect of the hydrogen chloride contained in the aramid fibres svm, armos, and rusar on their properties during prolonged storage and use. *Fibre Chemistry*, 38(6):450–452, 2006.
- [18] *Accumet Excel XL Series Meters User Manual*. Fisher Scientific, 1st edition, 2006.
- [19] *Vertex 80 User Manual*. Bruker Optics, Ettlingen, Germany, 1st edition, 2006.
- [20] L. M. Nollet. *Handbook of Water Analysis*. CRC Press, New York, 1st edition, 2000.
- [21] L. Penn and F. Larsen. Physicochemical properties of kevlar 49 fiber. *Journal of Applied Polymer Science*, 23:59–73, 1979.
- [22] A.M. Tiefenthaler and M.W. Urban. Surface studies of polymer films and fibers by circle atr ft-ir. *Applied Spectroscopy*, 42(1):163–166, 1988.
- [23] R. R. Gupta. *Physical Methods in Heterocyclic Chemistry*. General Heterocyclic Chemistry Series. John Wiley, New York, 1984.
- [24] R.M. Silverstein, G.C. Bassler, and T.C. Morrill. *Spectrometric Identification of Organic Compounds*. John Wiley and Sons, New York, 5th edition, 1991.
- [25] G. Socrates. *Infrared Characteristic Group Frequencies*. John Wiley, Chichester, 1980.
- [26] C. Cameron. *Enhanced Rates of Electron Transport in Conjugated-Redox Polymer Hybrids*. PhD thesis, Memorial University of Newfoundland, 2000.

REFERENCES

- [27] A. Suwaiyan, R. Zwarich, and N. Baig. Infrared and raman spectra of benzimidazole. *Journal of Raman Spectroscopy*, 21:243–249, 1990.